Electronic Supplementary Information for Dalton Transactions

Supporting Information

Switching and Fluorescence Signal Amplification with Metal Ions in Allosteric Systems Based on 1, 3-*Alternate* Thiacalix[4]crown

Manoj Kumar, Vandana Bhalla, Abhimanew Dhir*

Department of Chemistry, UGC Centre for Advanced Studies,

Guru Nanak Dev University, Amritsar, Punjab -143005- INDIA

25,27-Bis[2-(anthracenyl)iminoethoxy]-26,28-dipropyloxythiacalix[4]arene in 1,3-alternate conformation[7]:

To a solution of diamine **6** (0.10 g, 0.11 mmol) in a 1:1 mixture of chloroform and methanol (20 mL) was added a solution of 9-anthracene carbaldehyde (0.048 g, 0.21 mmol) in methanol (5 mL). The mixture was stirred for 24 h to separate a solid, which was filtered, washed and recrystallized from chloroform and methanol. The compound **4** was obtained in 81 % yield (0.115 g,) mp. 235°c.; νmax (KBr pellet, cm^{-1}) 1635 cm^{-1}; ; ^{1}H NMR ($CDCl_3$, 300 MHz): δ = 1.26 [s, 18 H, $C(CH_3)_3$], 1.32 [s, 18 H, $C(CH_3)_3$], 0.67 [t, *J* = 6.9 Hz, 6 H, CH_3], 1.072 -1.186 [m, 4H, CH_2], 3.66 [t, *J* = 7.2 Hz, 4H, NCH_2], 3.90 [t, *J* = 7.5 Hz, 4 H, OCH_2], 4.45 [t, *J* = 8.25 Hz, 4H, OCH_2], 7.39 [s, 4H, ArH], 7.58 [s, 4H, ArH], 7.30 – 7.50 (m, 8H, ArH), 7.99 [d, *J* = *8.1*, 4H, ArH], 8.43 [d, *J* = *8.4*, 4H, ArH], 8.49 [s, 2H, ArH], 9.45 [s, 2H, HC = N]; FAB-MS m/z 1267 $(M+1)^+$; Elemental Analysis Calcd for $C_{80}H_{86}N_2O_4S_4$: C, 75.82 % ; H, 6.95 % ; N, 2.21 % ; Found: C, 75.47 % ; H, 6.85 % ; N, 2.10%.

25,27-Bis[2-(anthracenyl)iminoethoxy]-26,28-dipropyloxythiacalix[4]arene in 1,3-alternate conformation[8]:

To a solution of diamine **6** (0.10 g, 0.11 mmol) in a 1:1 mixture of chloroform and methanol (20 mL) was added a solution of 2-quinoline carboxaldehyde (0.037 g, 0.21 mmol) in methanol (5 mL). The mixture was stirred for 24 h to separate a solid, which was filtered, washed and recrystallized from chloroform and methanol. The compound **8** was obtained in 83% yield (0.11 g,) mp. 242°c; ν_{max} (KBr pellet, cm^{-1}) 1635 cm^{-1}; ^{1}H NMR ($CDCl_3$, 300 MHz): δ = 1.26 [s, 18 H, $C(CH_3)_3$], 1.31 [s, 18 H, $C(CH_3)_3$], 0.65 [t, *J* = 7.5 Hz, 6H, CH_3], 1.08 -1.27 [m, 4H, CH_2], 3.40 [t, *J* = 7.5 Hz, 4H, NCH_2], 3.87 [t, *J* = 7.5 Hz, 4H, OCH_2], 4.25 [t, *J* = 7.5 Hz, 4H, OCH_2], 7.27 [s, 4H, ArH], 7.33 [s, 4H, ArH], 7.50 – 7.70 (m, 2H, ArH), 7.71 – 7.74 (m, 2H, ArH),7.82 (d, *J* = *6 Hz*, 2H, ArH) 8.03 – 8.20 (m, 4H, ArH), 8.32 [d, *J* = 9 Hz, 2H, ArH], 8.48 [s, 2H, HC = N]; FAB-MS m/z 1169 $(M+1)^+$; Elemental Analysis Calcd for $C_{82}H_{88}N_2O_7S_4$: C, 71.92 % ; H, 6.84 % ; N, 4.79 % ; Found: C, 71.97 % ; H, 6.66 % ; N, 4.59 %.

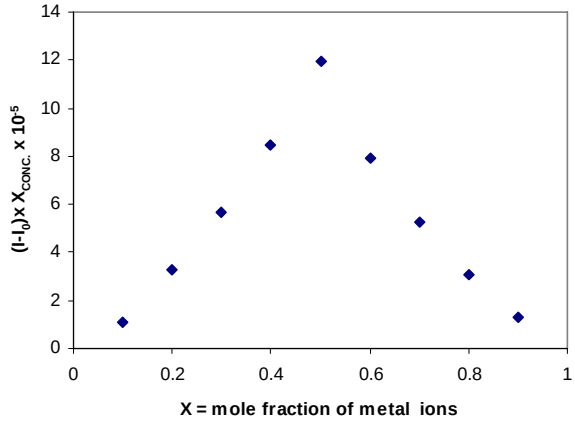

Figure S1. Job's plot of **4** with $\mathbf{Fe^{3+}}$ representing stoichiometry 1:1 (host: guest).

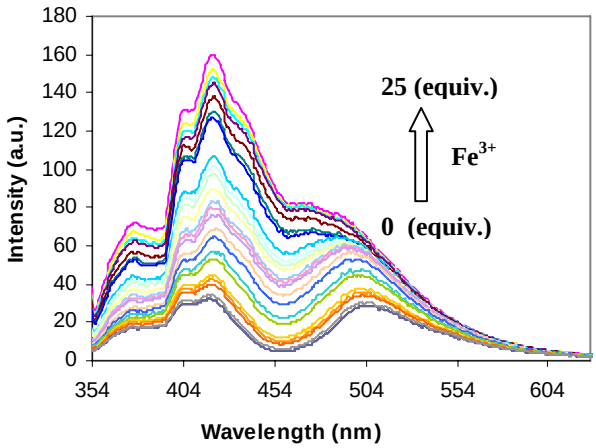

Figure S2. Fluorescence spectra of **7** (1 X 10^{-5} M) in response to the presence of $\mathbf{Fe^{3+}}$ ions (25 equiv.) in THF; λ_{ex} = 340 nm

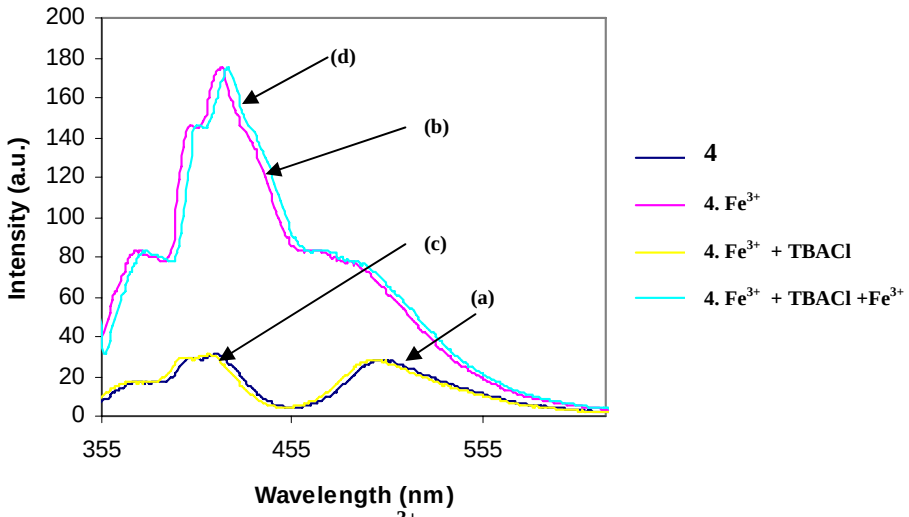

Figure S3. Reversibility of Fe^{3+} coordination to **4** by Tetrabutyl ammonium chloride (TBACl). (a) **4** (1 X 10^{-5} M); (b) **5** + 20 equiv. Fe^{3+}; (c) **4** + 20 equiv. Fe^{3+} + 12 equiv. (TBACl); (d) **4** + 20 equiv. Fe^{3+} + 12 equiv. (TBACl) + 30 equiv. Fe^{3+}.

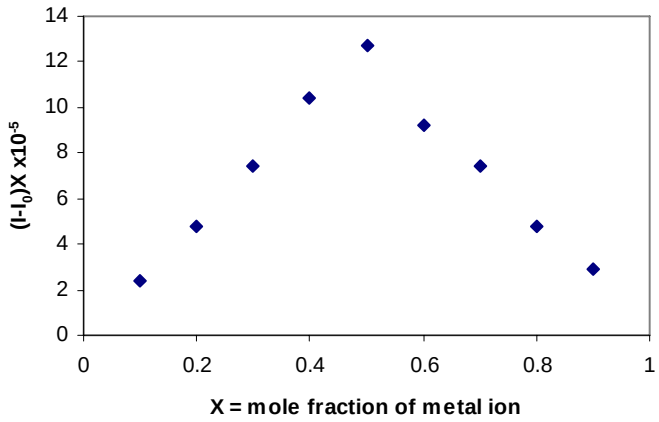

Figure S4. Job's plot of **5** with Hg^{2+} representing stoichiometry 1:1 (host: guest).

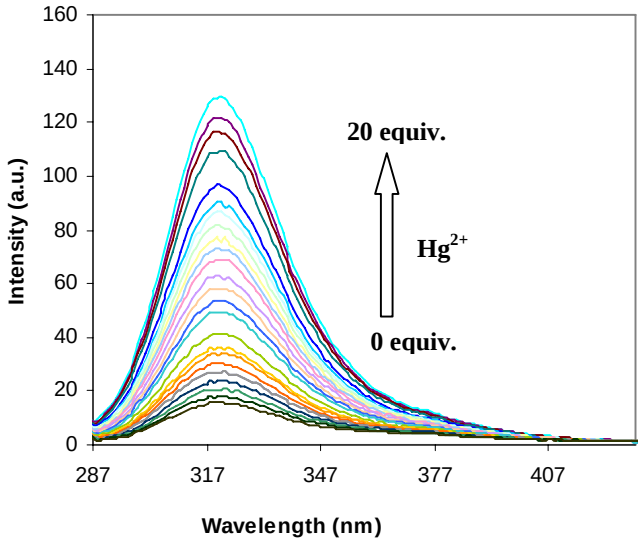

Figure S5. Fluorescence spectra of **8** (1×10^{-5} M) in response to the presence of $\mathbf{Hg^{2+}}$ ions (20 equiv.) in THF; λ_{ex} = 245 nm.

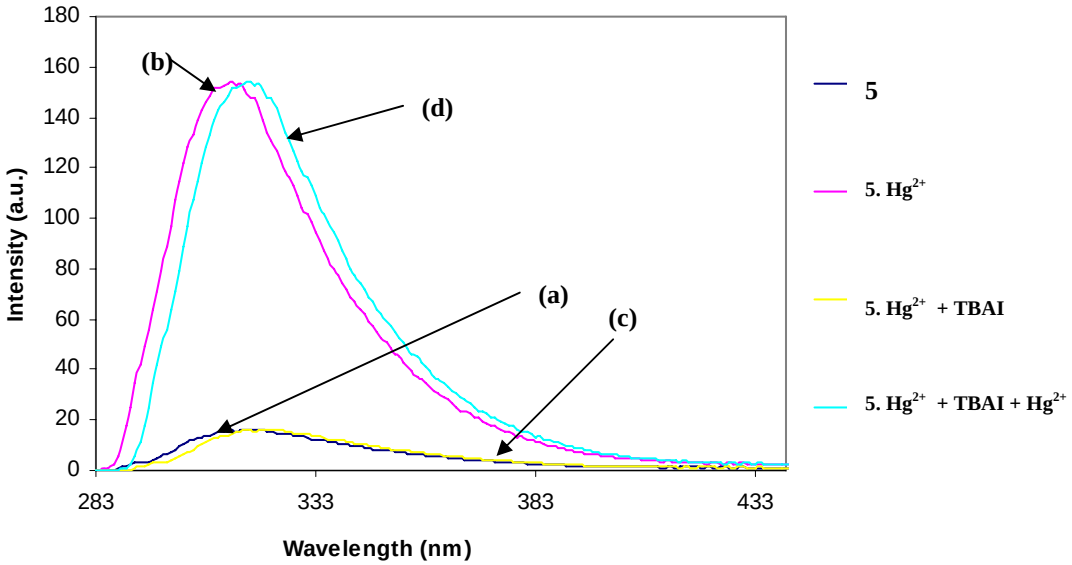

Figure S6. Reversibility of Hg^{2+} coordination to **5** by Tetrabutyl ammonium iodide (TBAI). (a) **5** (1 X 10^{-5} M); (b) **5** + 16 equiv. Hg^{2+}; (c) **5** + 16 equiv. Hg^{2+} + 15 equiv. (TBAI); (d) **5** + 16 equiv. Hg^{2+} + 15 equiv. (TBAI) + 20 equiv. Hg^{2+}.

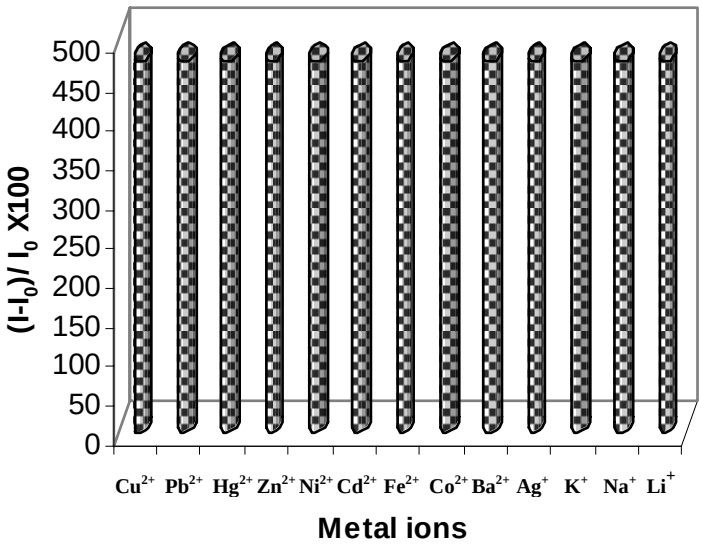

Figure S7. Fluorescent response of sensor **4** (1 X 10^{-5} M) to **Fe^{3+}** (20 equiv.) ions over other selected metal ions (100 equiv.).

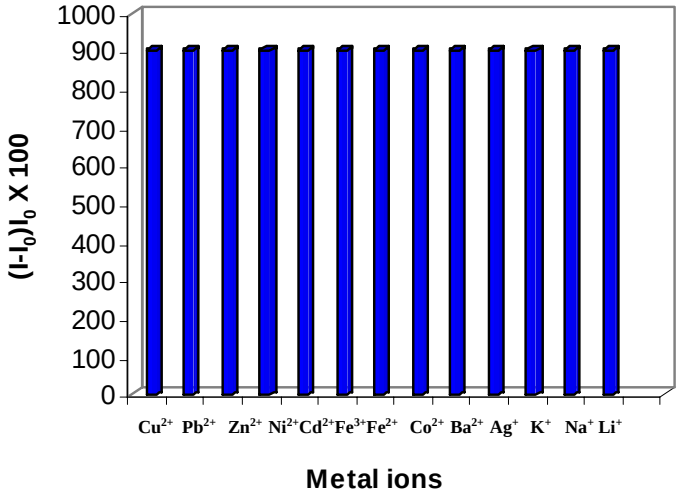

Figure S8. Fluorescent response of sensor **5** (1 X 10^{-5} M) to Hg^{2+} (16 equiv.) ions over other selected metal ions (100 equiv.).

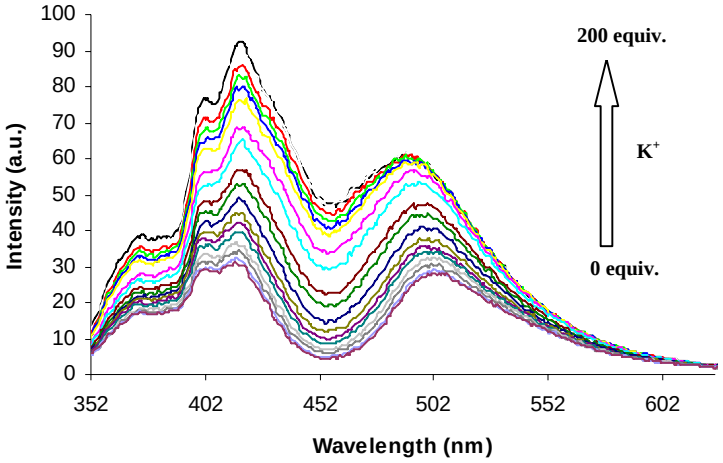

Figure S9. Fluorescence spectra of **4** (1 X 10^{-5} M) in response to the presence of $\mathbf{K}^+$ ions (200 equiv.) in THF; λ_{ex} = 340 nm.

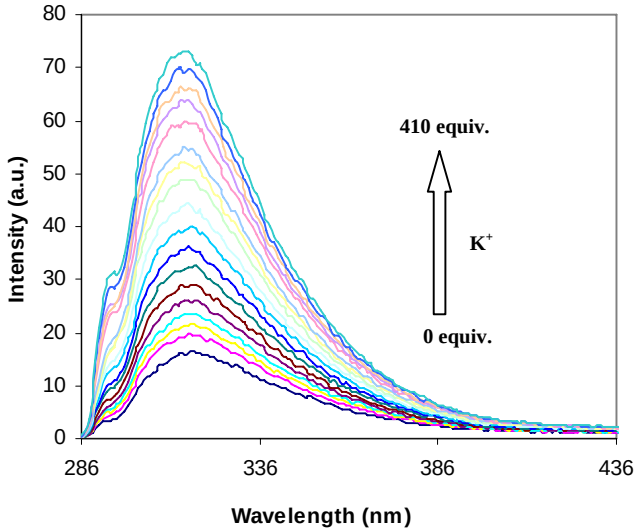

Figure S 10. Fluorescence spectra of **5** (1 X 10^{-5} M) in response to the presence of $\mathbf{K}^+$ ions (410 equiv.) in THF; λ_{ex} = 245 nm.

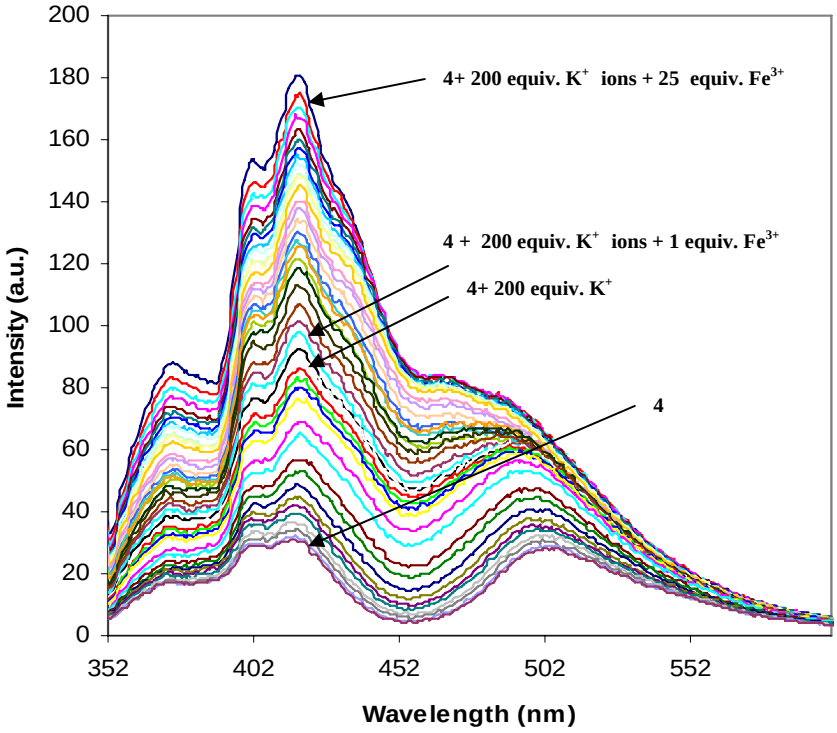

Figure S11. Fluorescence emission spectra of **4** (1 X 10^{-5} M) on addition of K^+ ions (200 equiv.) and further addition of Fe^{3+} ions (25 equiv.) .

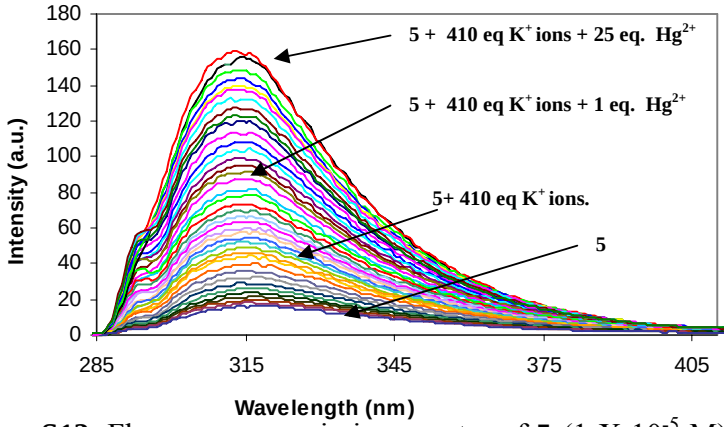

Figure S12. Fluorescence emission spectra of **5** (1 X 10^{-5} M) on addition of K^+ ions (410 equiv.) and further addition of Hg^{2+} ions (25 equiv.).

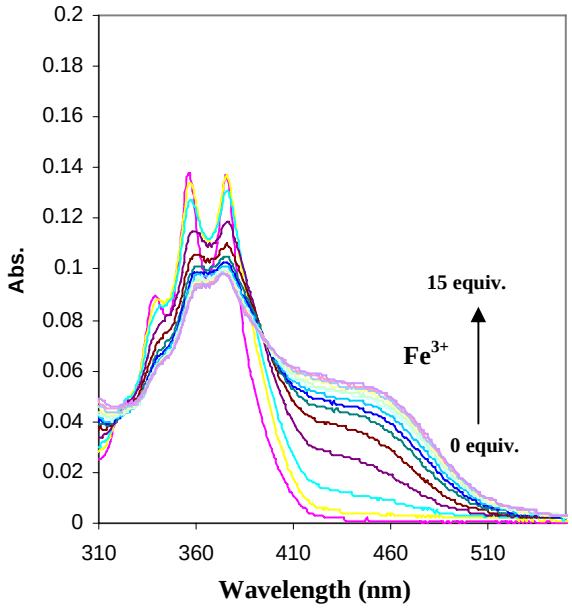

Figure S13. UV-vis spectra of **4** (1 X 10^{-5} M) in response to the presence of $\mathbf{Fe^{3+}}$ ions (15 equiv.) in THF.

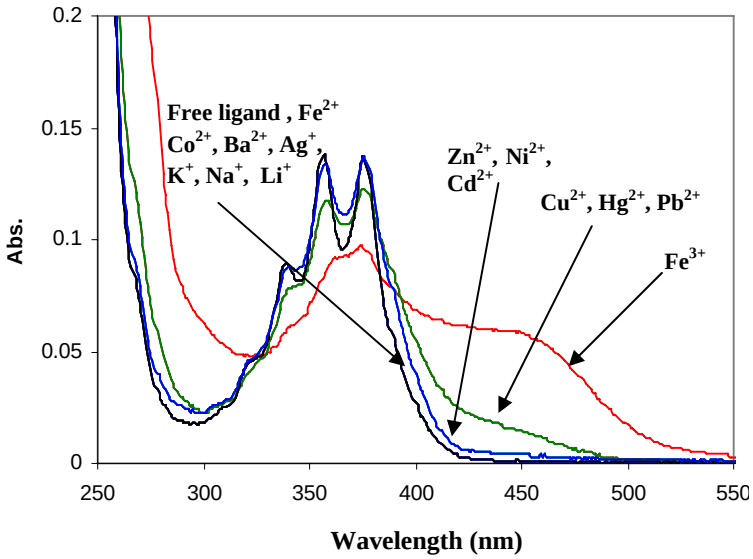

Figure S14. UV-vis spectra of **4** (1 X 10^{-5} M) in response to the presence of various metal ions (15 equiv.) in THF.

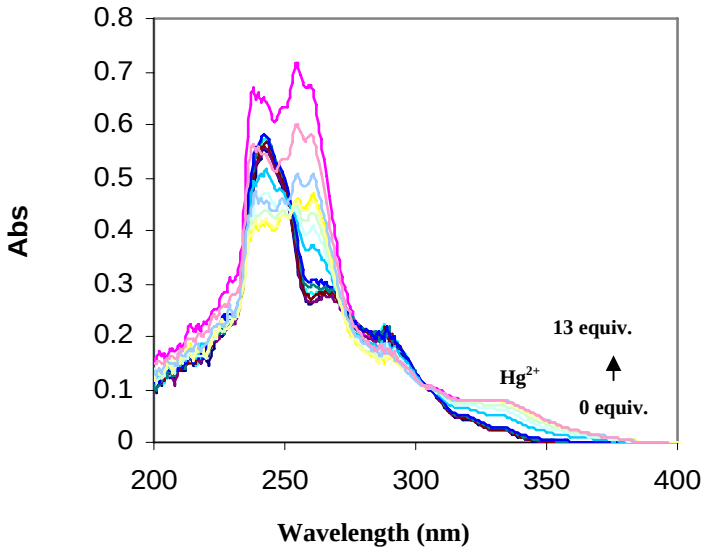

Figure S15. UV-vis spectra of **5** (1 X 10^{-5} M) in response to the presence of **Hg^{2+}** ions (13 equiv.) in THF.

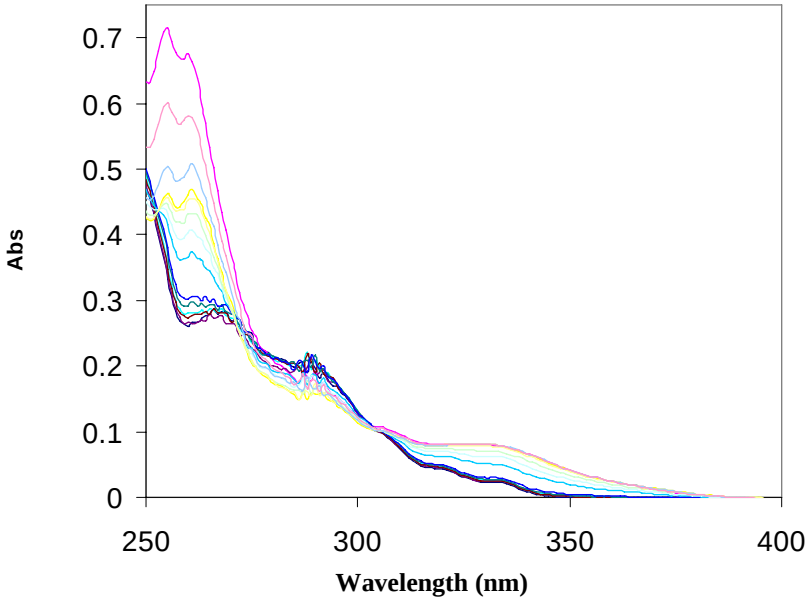

Figure S15. Figure Magnified view of above figure.

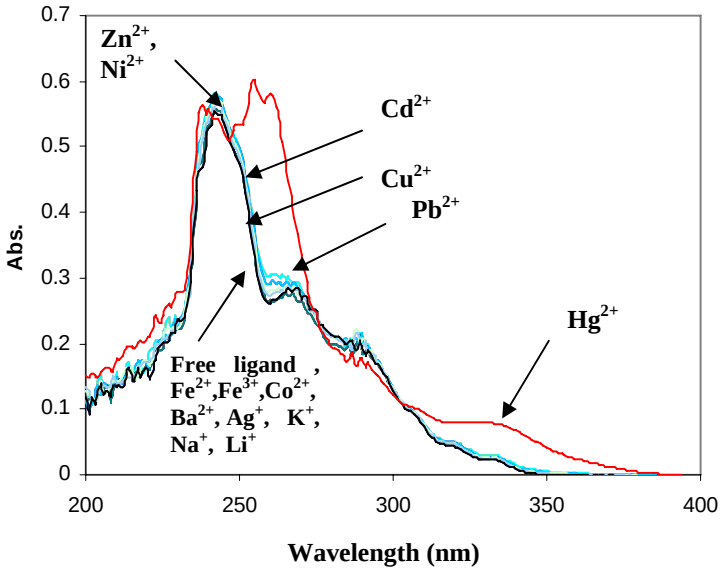

Figure S16. UV-vis spectra of **5** (1 X 10^{-5} M) in response to the presence of ions various metal ions (13 equiv.) in THF.

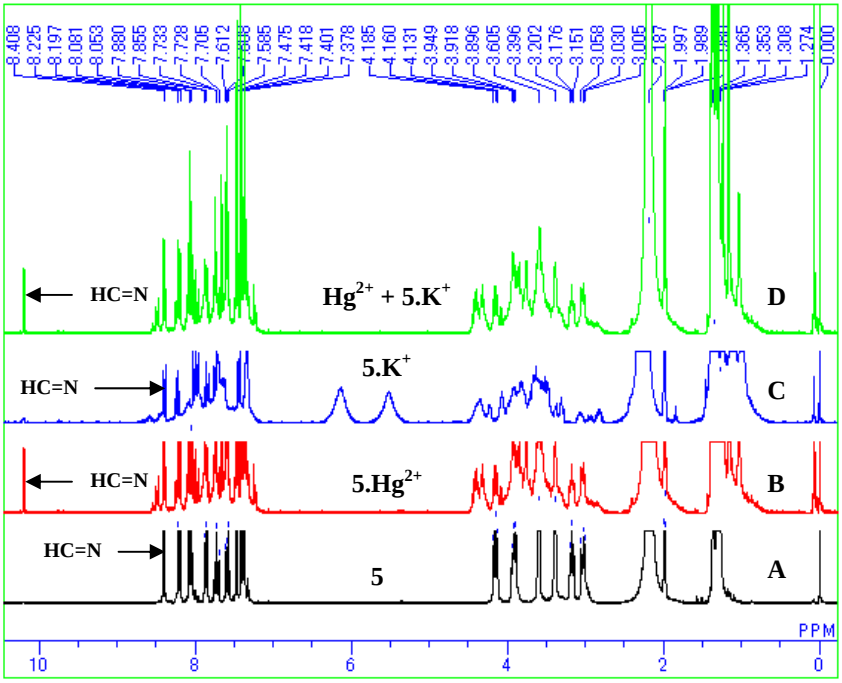

Figure S17. ^{1}H NMR spectra of **5** in $CDCl_3/CD_3CN$ (8:2). **(A)** Free ligand **(B)** in presence of 1.0 equiv of mercury perchlorate; **(C)** in presence of 1.0 equiv of potassium perchlorate; **(D)** addition of 1.0 equiv of mercury perchlorate to ligand/potassium complex. NMR frequency is 300 MHz.

Figure S18. ^{1}H NMR Spectrum of 4

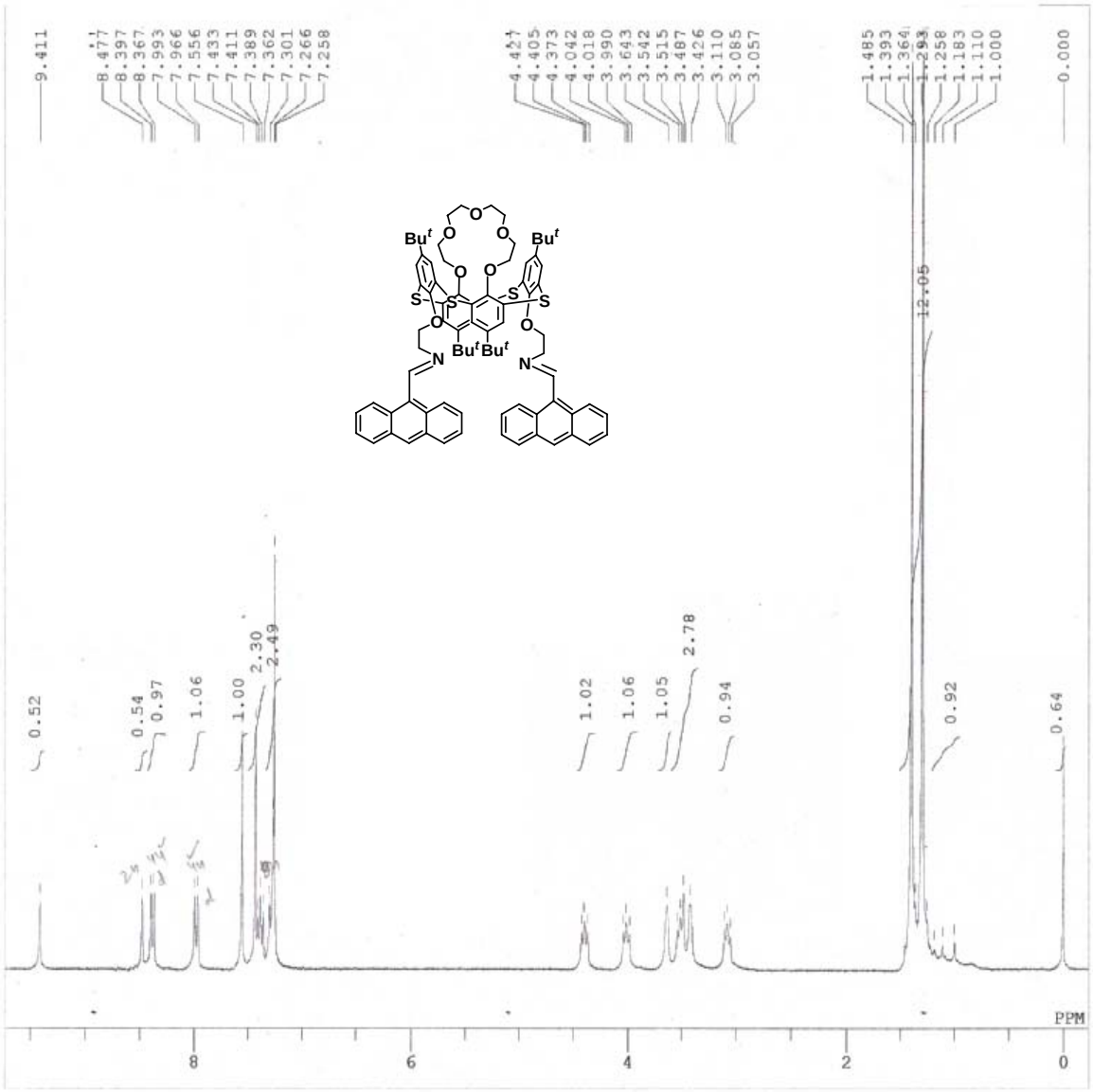

Figure S19. ^{13}C NMR Spectrum of 4

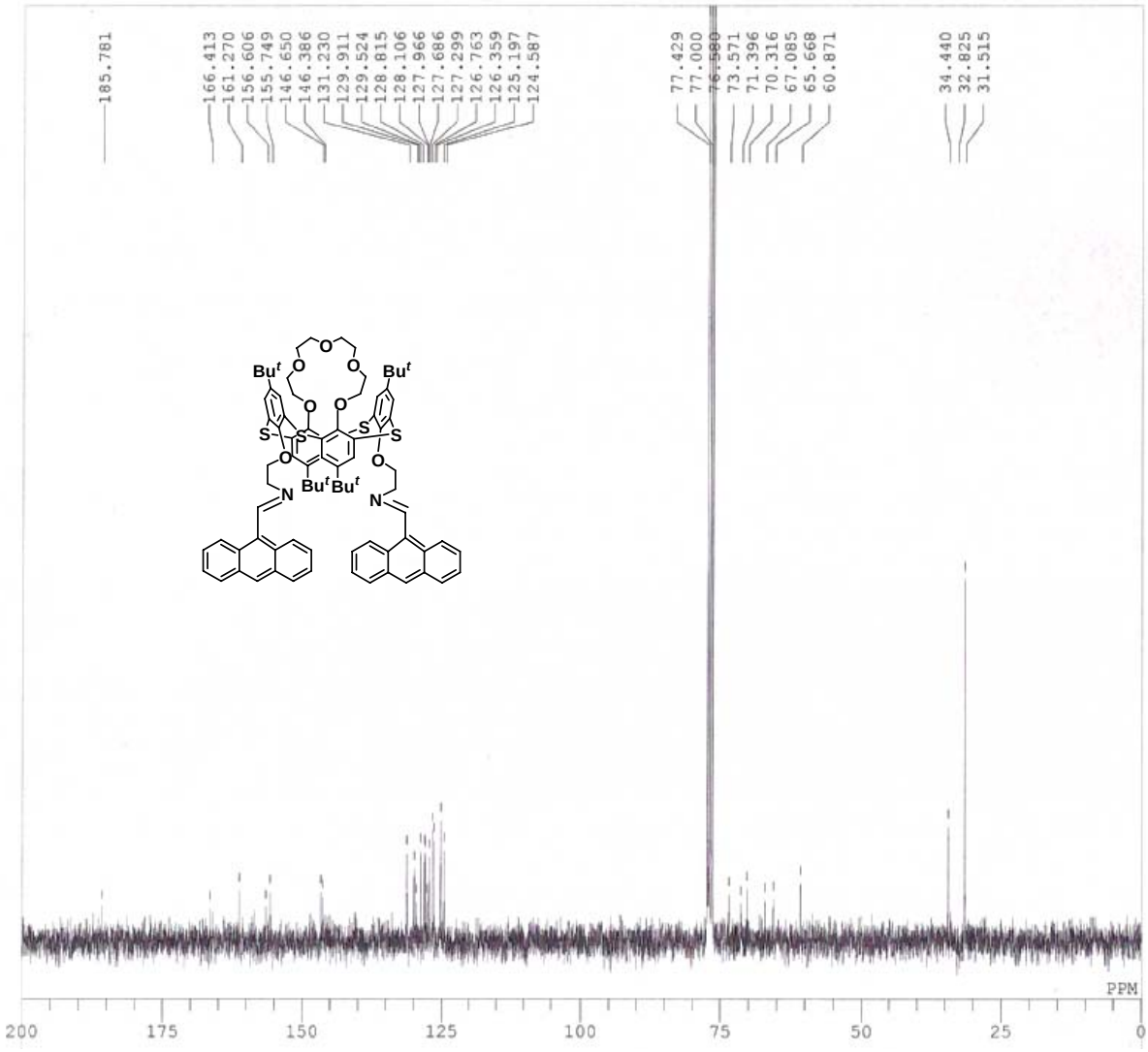

Figure S20. Mass Spectrum of 4

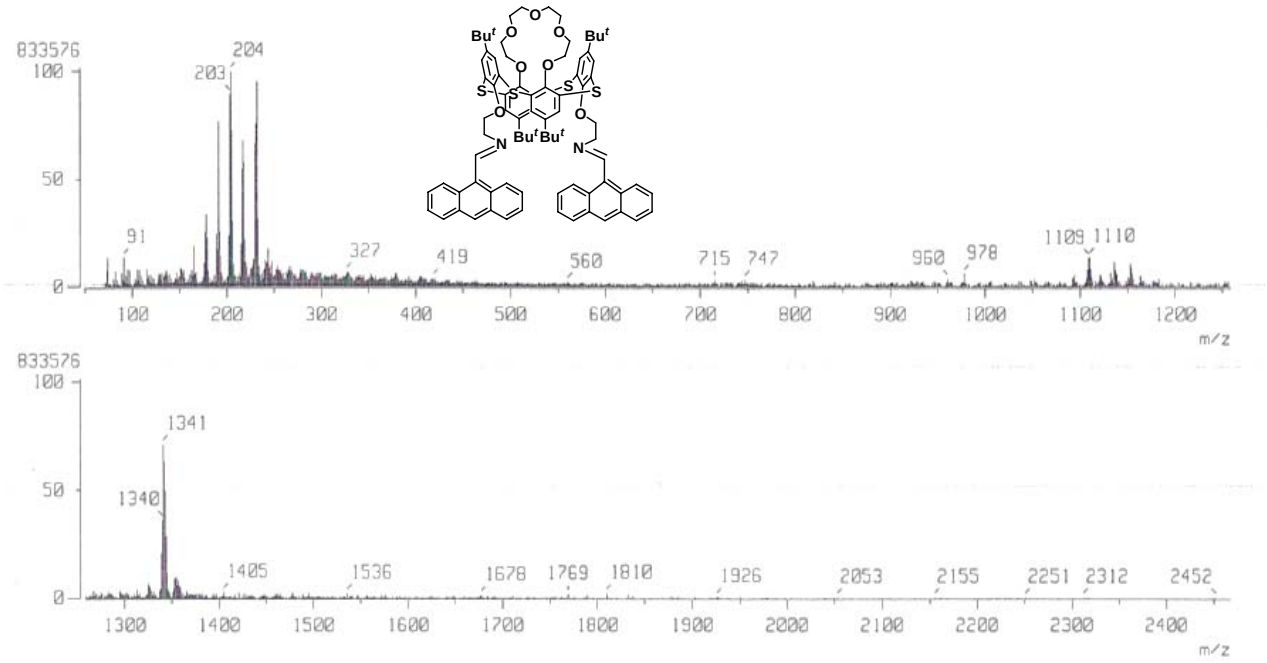

Figure S21. ^{1}H NMR Spectrum of 5

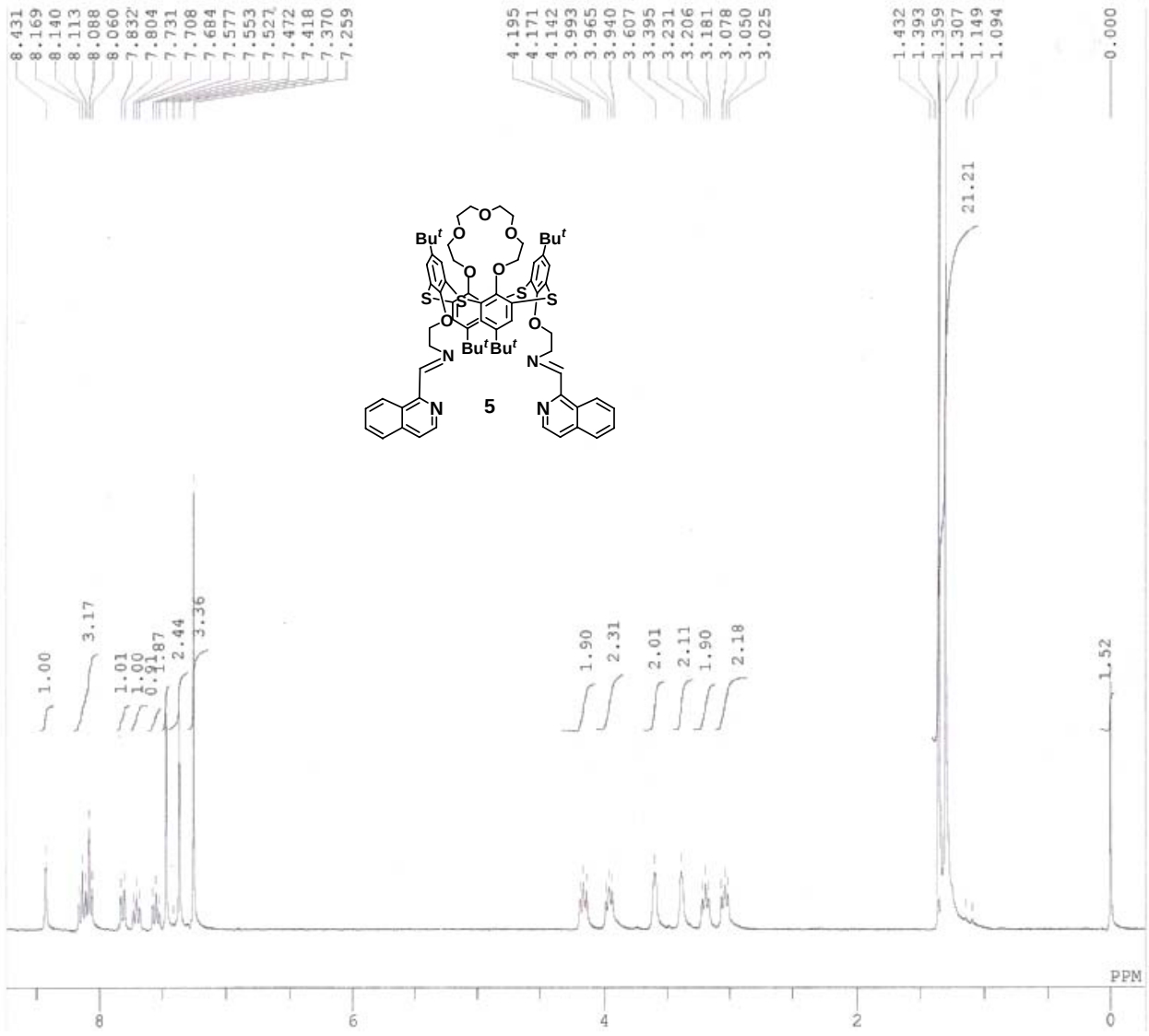

Figure S22. ^{13}C NMR Spectrum of 5

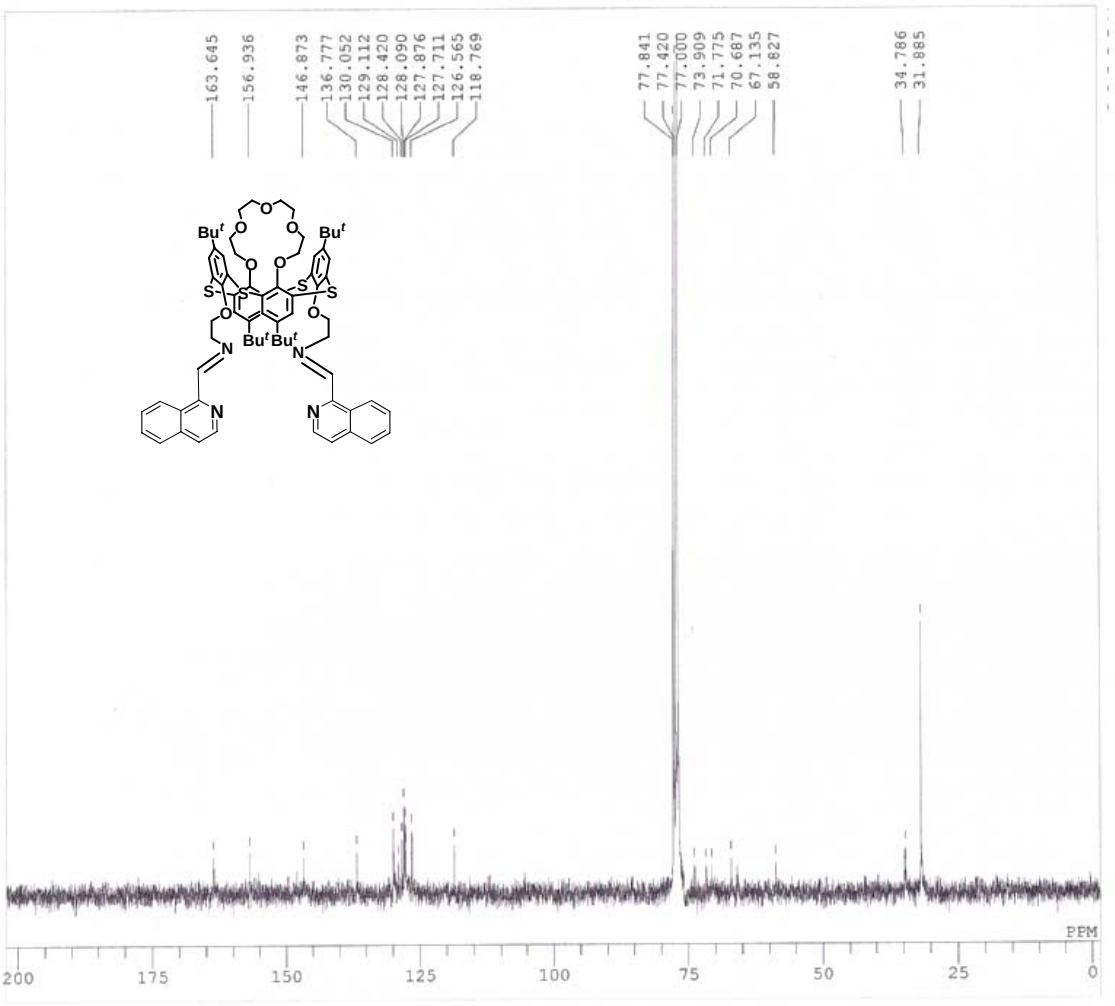

Figure S23. Mass Spectrum of 5

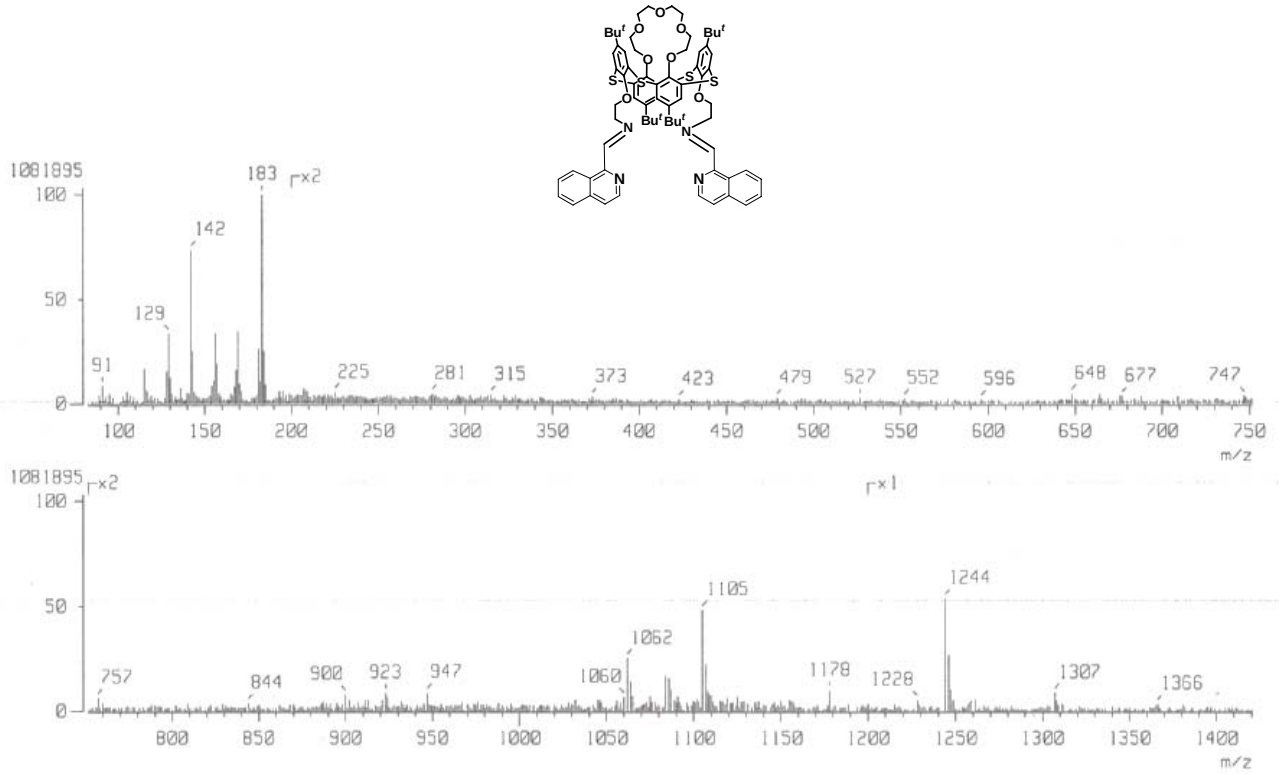

Figure S24. ^{1}H NMR Spectrum of 7

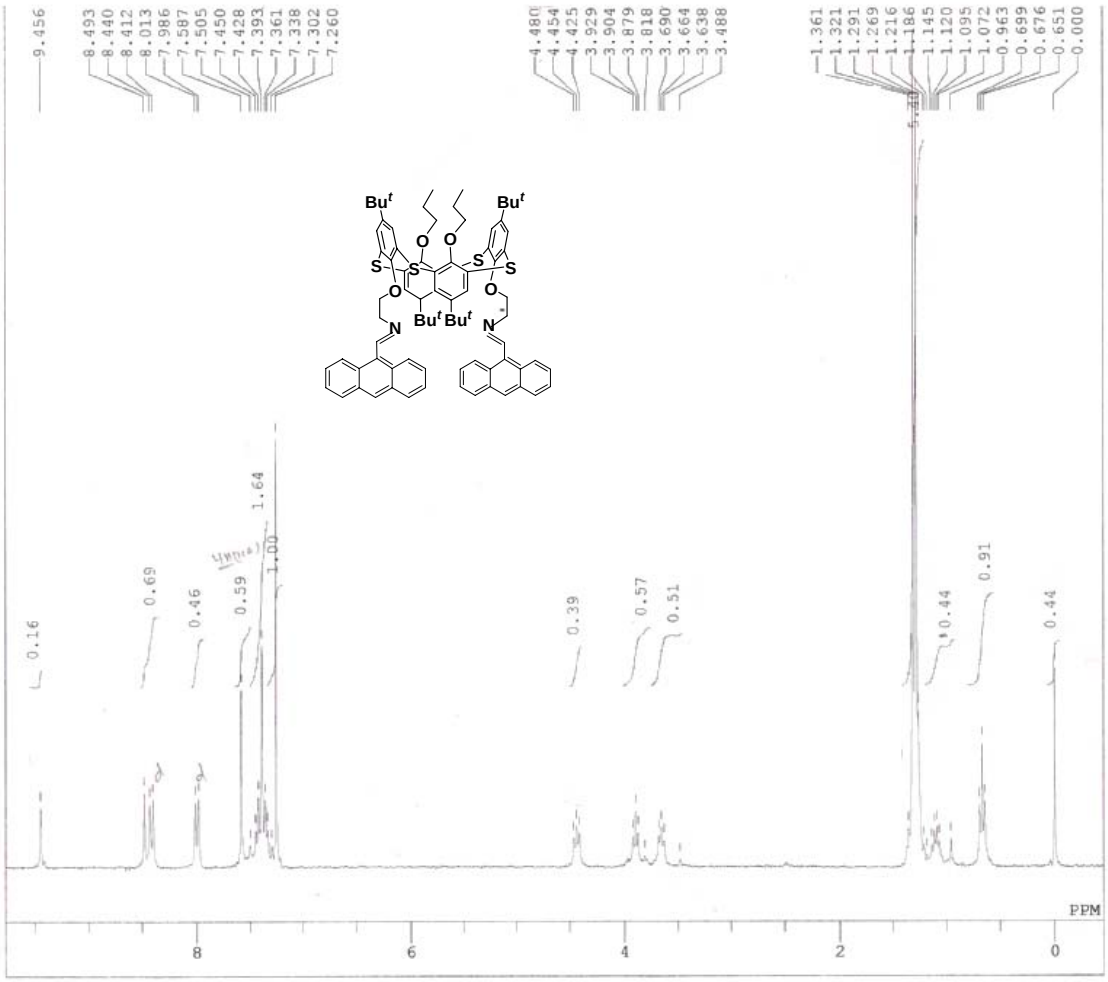

Figure S25. Mass Spectrum of 7

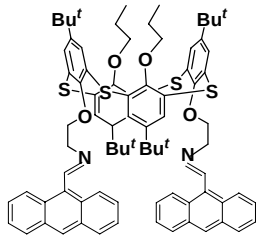

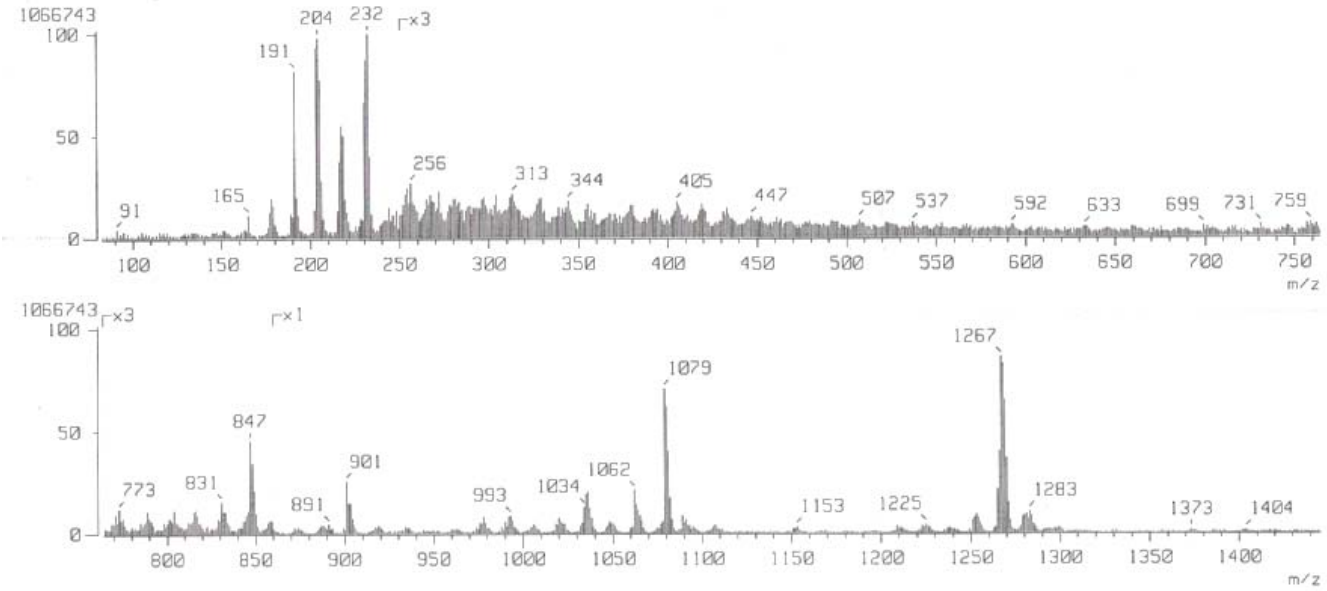

Figure S26. ^{1}H NMR Spectrum of 8

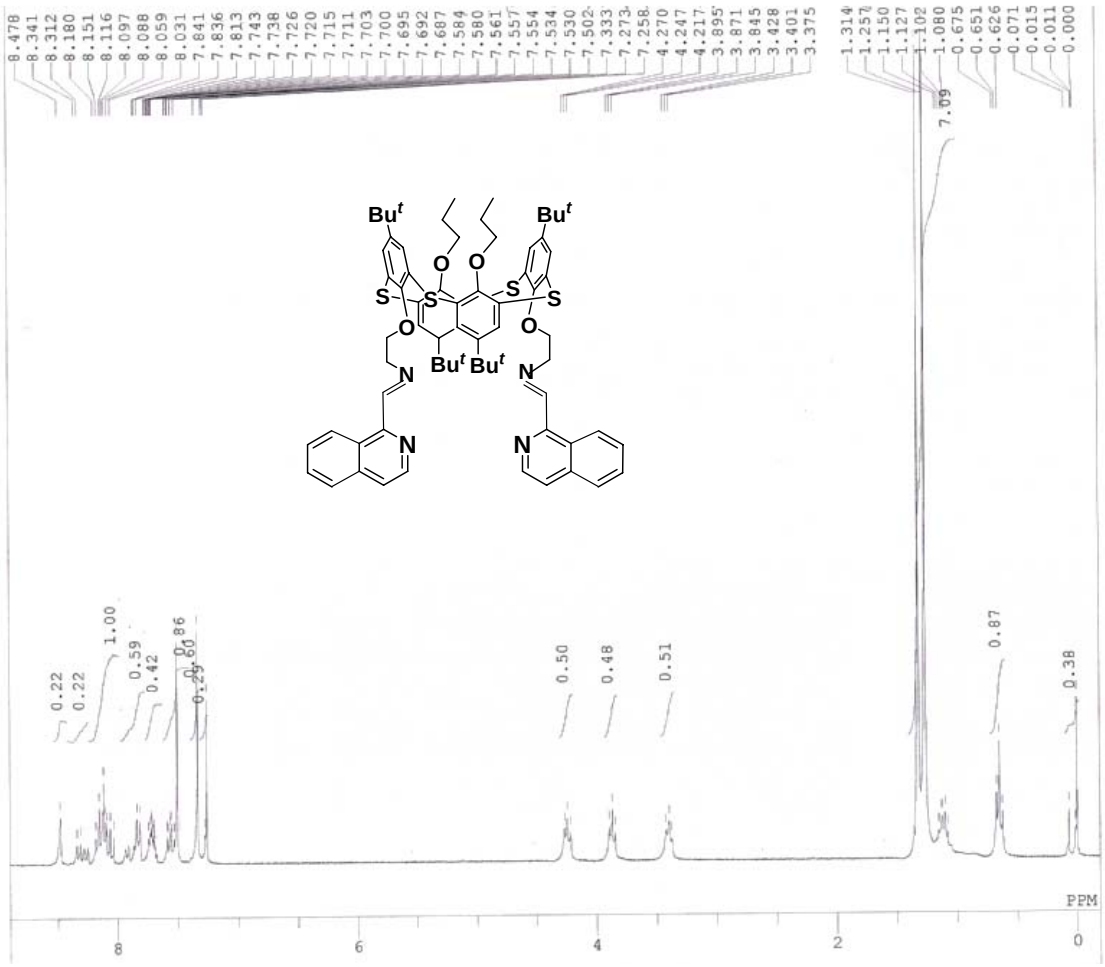

Figure S27. Mass Spectrum of 8

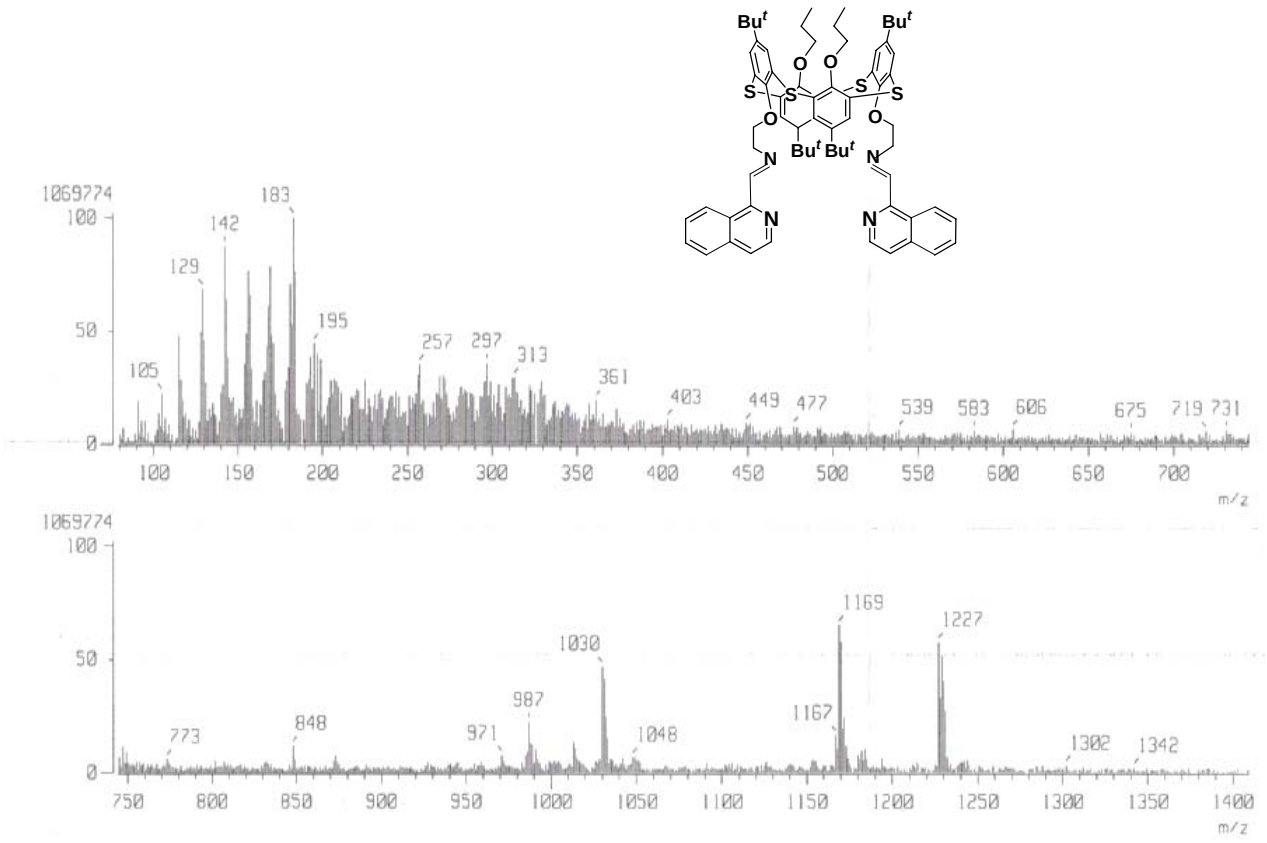

Figure S28. IR Spectrum of 4

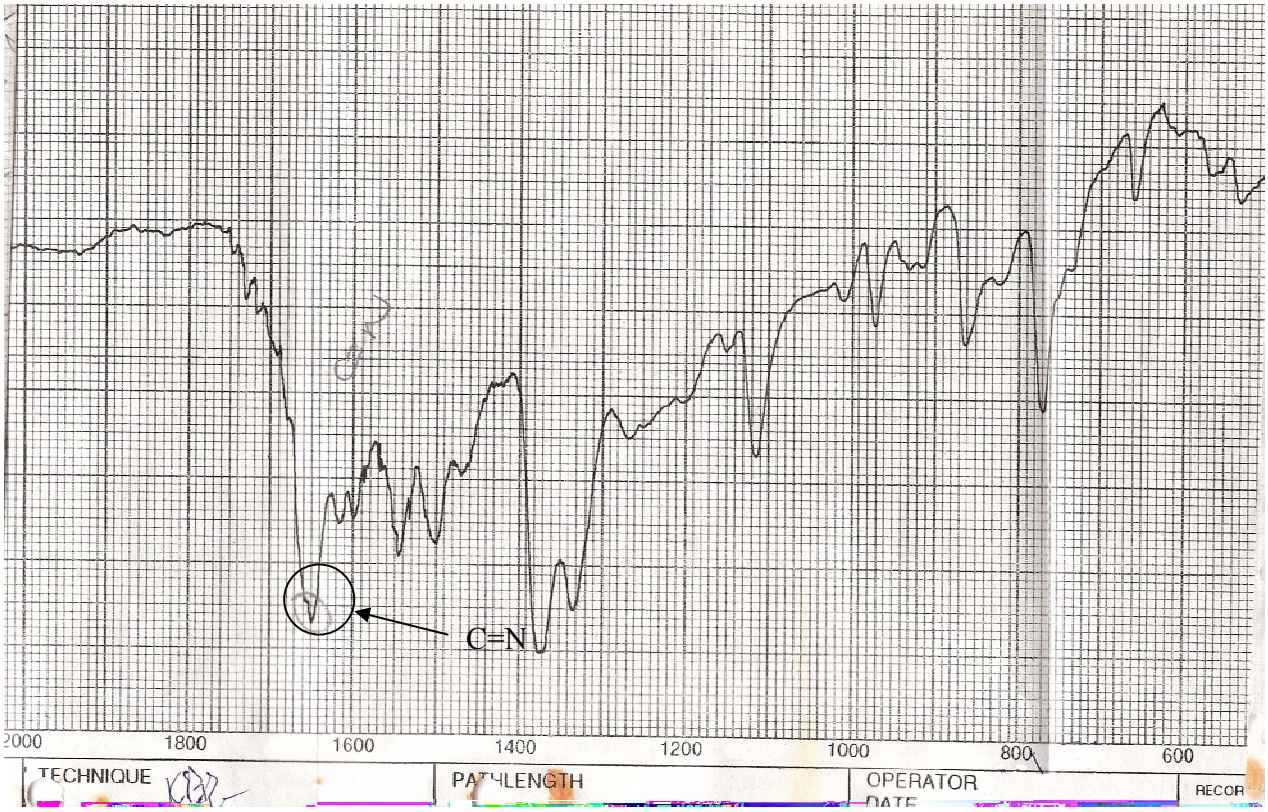

Figure S29. IR Spectrum of 5

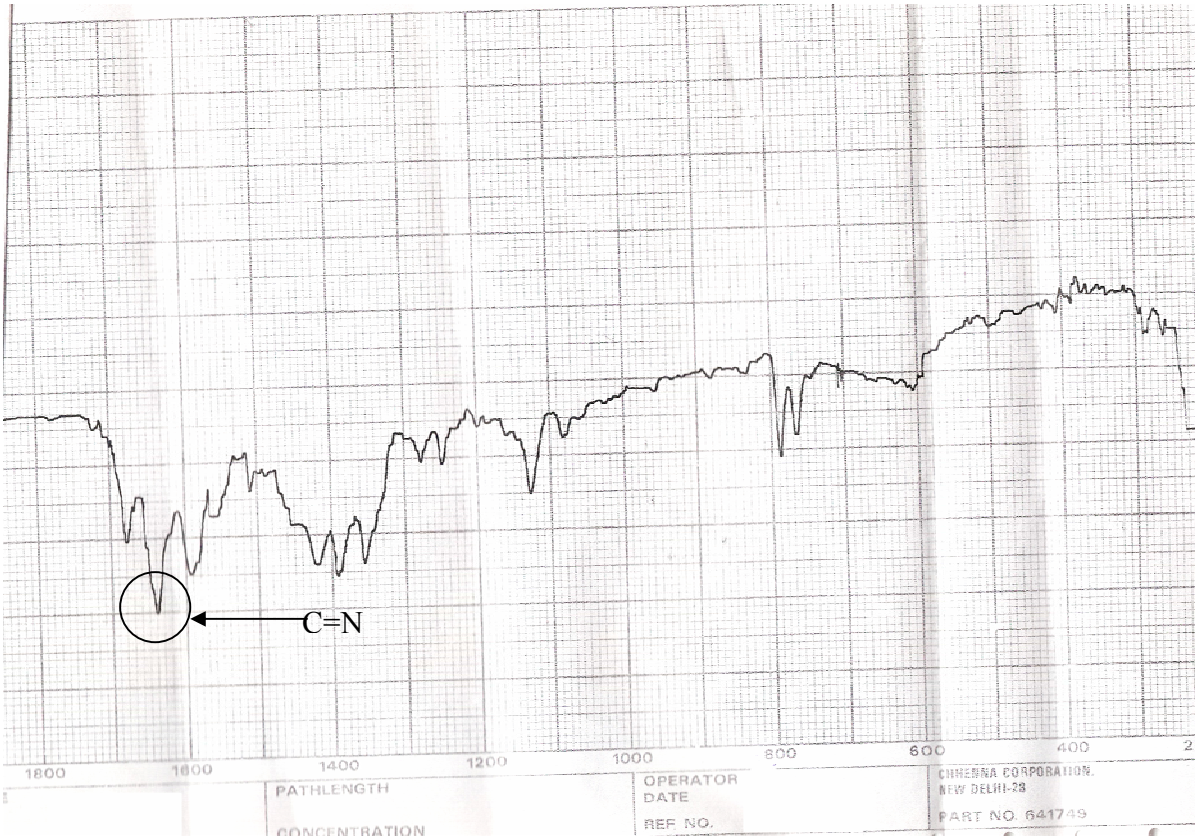

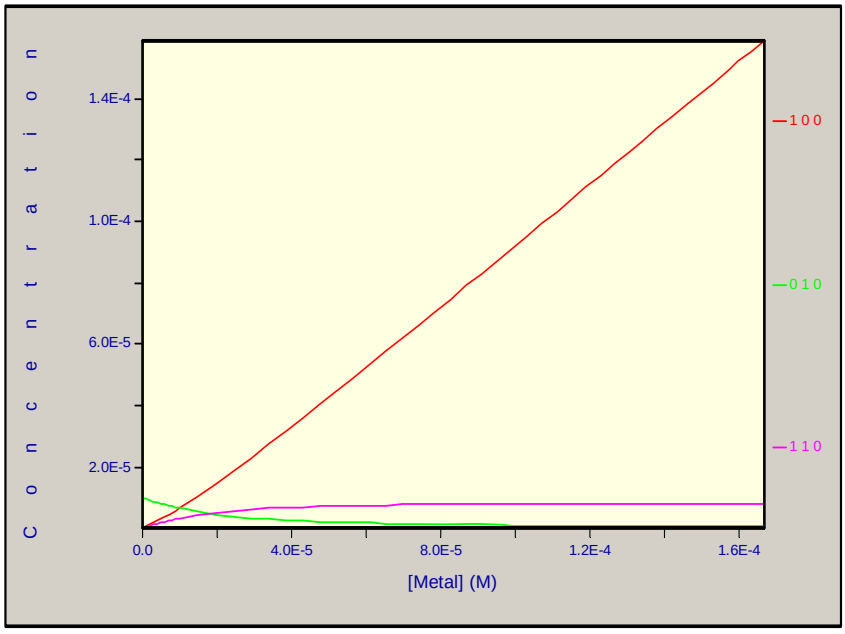

Figure S30. Concentration plot for 4.Fe^{3+} obtained from SPECFIT.

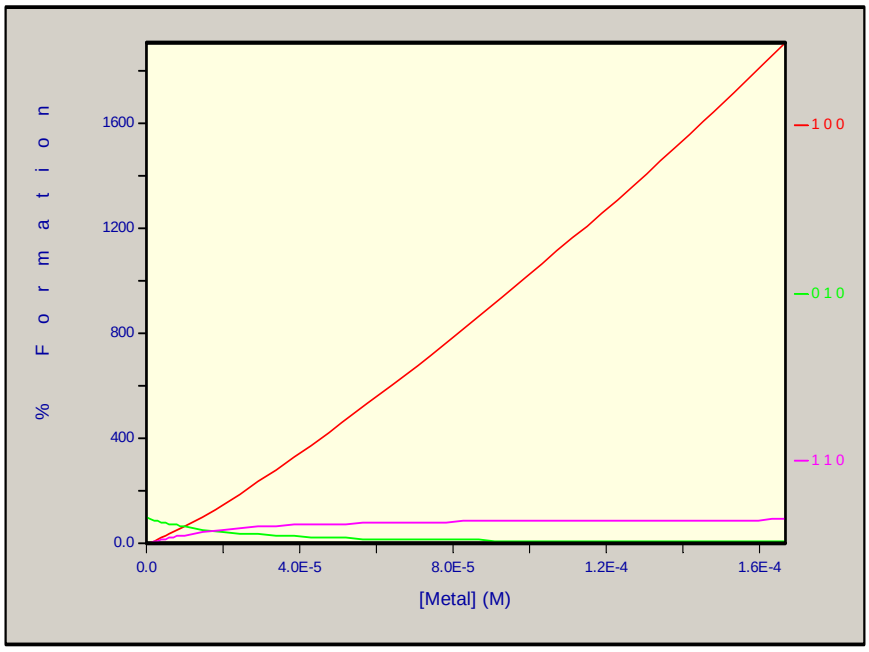

Figure S31. Percent complex formation plot of 4.Fe^{3+} for obtained from SPECFIT.

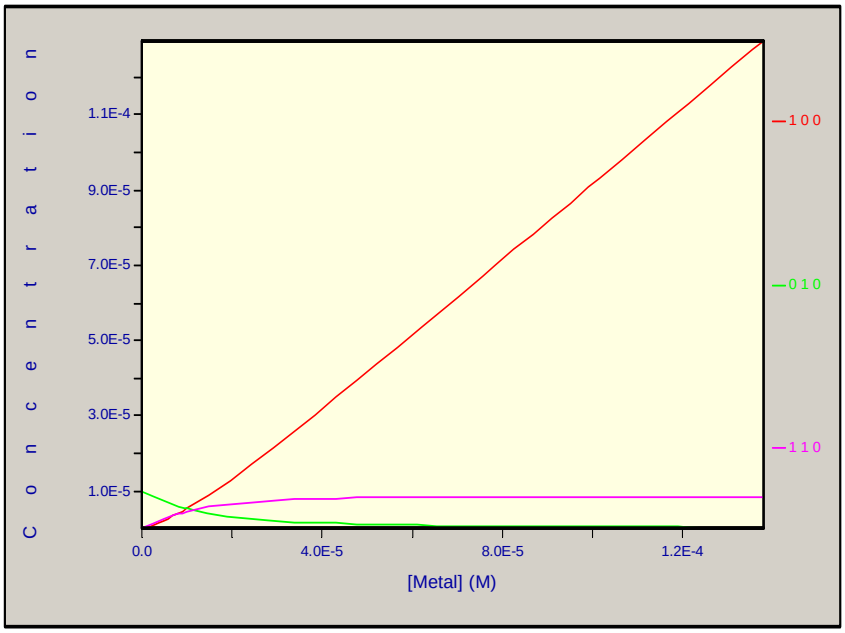

Figure S32. Concentration plot for 5.Hg^{2+} obtained from SPECFIT.

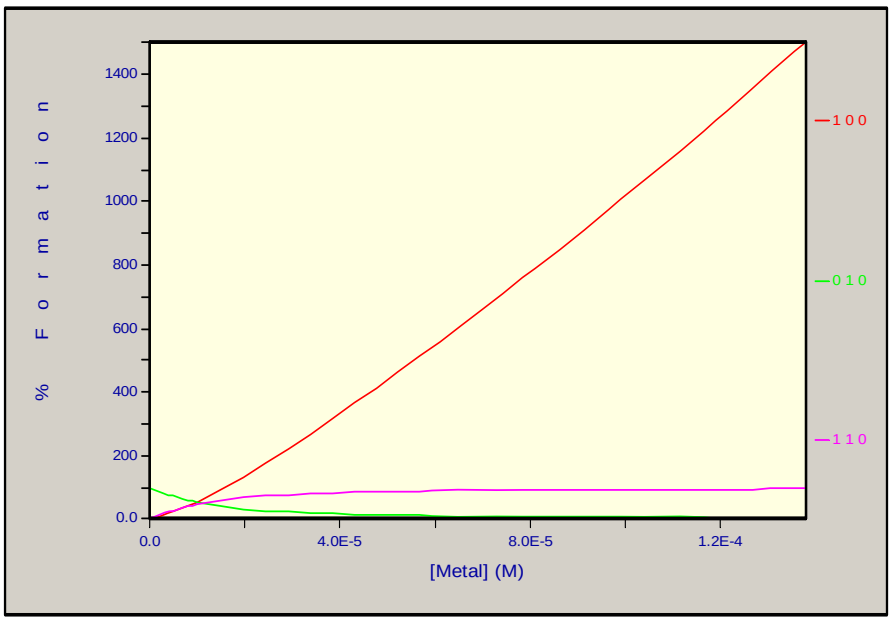

Figure S33. Percent complex formation lot for 5.Hg^{2+} obtained from SPECFIT.

Table S1 for Quantum Yield.

	Absorbance taken for QY at excitation wavelength A_S	Qy of Sample (ϕ_s)
4 in free state	0.088	0.013
4.Fe^{3+} complex	0.061	0.094
5 in free state	0.065	0.023
5.Hg^{2+} complex	0.063	0.188

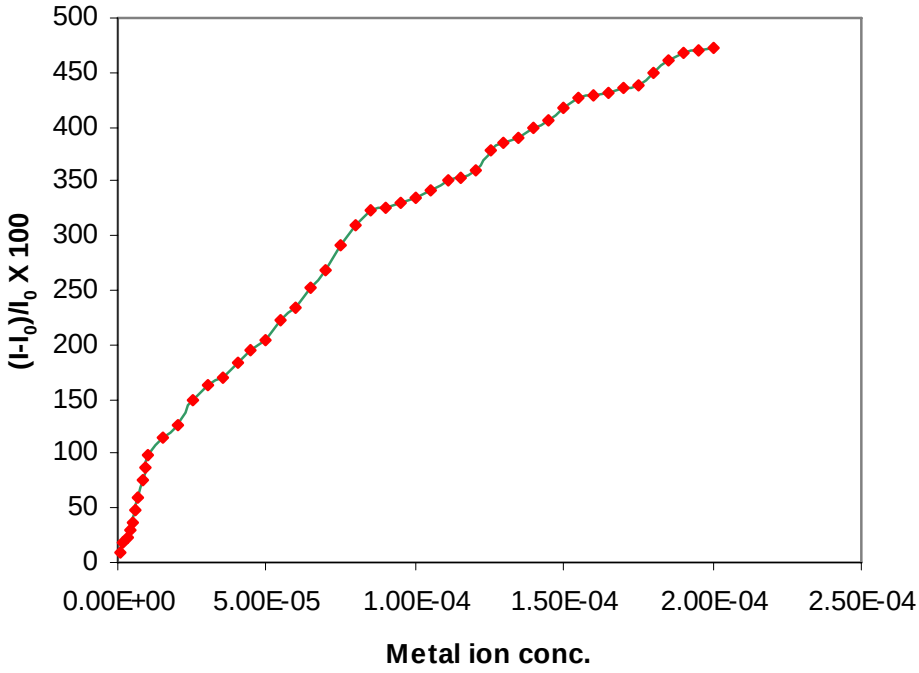

Figure S34. Curve fitting for 4.Fe^{3+} complex with respect to experimental data.

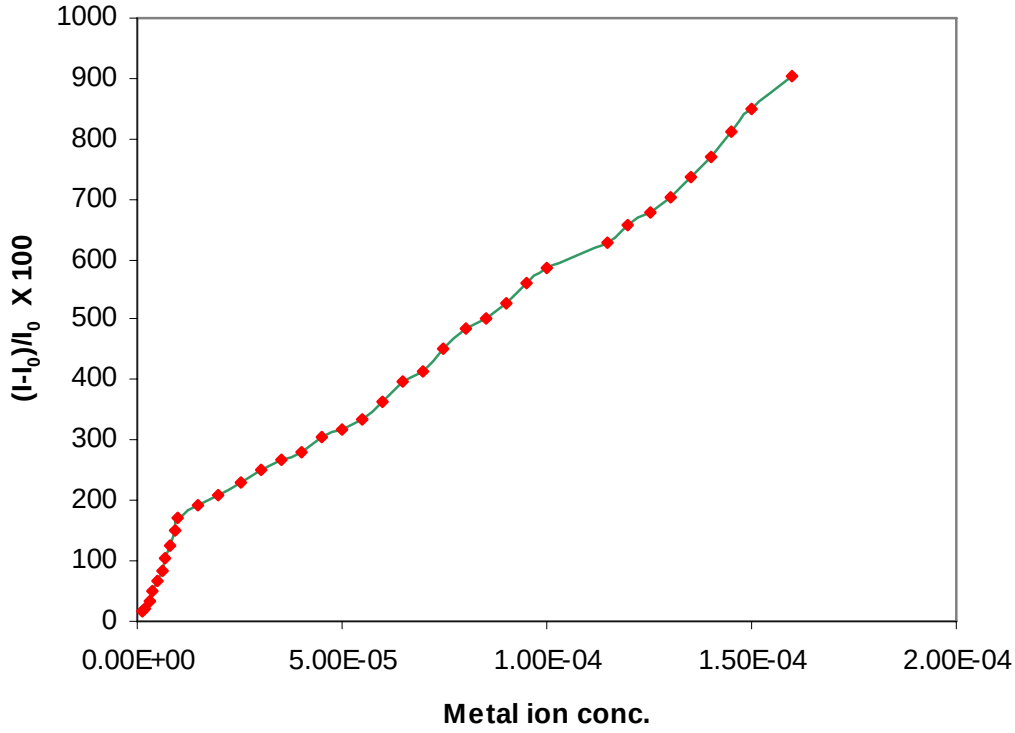

Figure S35. Curve fitting for 5.Hg^{2+} complex with respect to experimental data.